I. Solekhudin and K.C. Ang/ Electronic Journal of Boundary Elements, Vol. 10, No. 2, pp. 42-55 (2012)

Suction Potential and Water Absorption from Periodic Channels in Different Types of Homogeneous Soils

I. Solekhudin[1,2] and K. C. Ang[1]

[1]Mathematics and Mathematics Education
National Institute of Education
Nanyang Technological University, Singapore

[2]Department of Mathematics
Faculty of Mathematics and Natural Sciences
Gadjah Mada University, Indonesia

Abstract

In this paper, problems involving infiltration from periodic identical trapezoidal channels into homogeneous soils with root water uptake are considered. The governing equation of infiltration through soil is transformed to a modified Helmholtz equation using Kirchoff transformation with dimensionless variables. A DRBEM with a predictor-corrector scheme is employed to obtain numerical solutions to the modified Helmholtz equation. The proposed method is used to solve infiltration problems in three different types of soil. Results are shown to be physically meaningful.

Keywords : Richard's equation, Helmholtz equation, DRBEM, predictor-corrector, infiltration, root water uptake.

1 Introduction

Many researchers have been studying the problem of water infiltration from irrigation channels in recent years. Weachter and Mandal investigated time-independent infiltration from a semicircular cylindrical trench [19]. Steady infiltration from irrigation channels has been studied by Azis et al [3], and Clements and Lobo [8]. Problems involving steady infiltration with impermeable inclusion have been considered by Lobo et al [11], while Clements et al [7] examined infiltration problems with impermeable layers. Lobo and Clements studied time-dependent infiltration from an irrigation channel with as well as without inclusions [12]. The study of the models of root water uptake has also been considered by researchers, such as Vrugt et al [17], Vrugt et al [18], Li et al [10], and Skaggs et al [14]. However, in most of these studies involving infiltration from irrigation channels, water absorption by plant roots was not taken into account.

In this paper, we investigate solutions to problems involving steady infiltration with absorption by plant roots in three different types of homogeneous soil. This study is a continuation of our previous study reported in [15]. For the convenience of readers and to ensure completeness of this paper, some basic equations and methods described in our previous study are briefly introduced.

A set of transformations is used to convert the governing equation to a modified Helmholtz equation. To solve the equation numerically, a numerical scheme based on a dual reciprocity boundary element method, or DRBEM, is constructed by employing an integral formulation. Using the DRBEM and a predictor-corrector scheme simultaneously, numerical solutions to the problems are obtained. The method is then applied to examine water infiltration in three different types of soil.

2 Problem Formulation

Using a Cartesian coordinate system $OXYZ$ with OZ vertically positive downwards, we consider three types of homogeneous soil, pima clay loam (PCL), touchet silt loam (TSL), and guelph loam (GL) in the region $Z \geq 0$. Periodic identical trapezoidal channels of $2L$ per unit length surface area are created on the surface of the soil. Crops, with roots of depth Z_m and width $2X_m$, are planted between and equidistant from two adjacent channels. The distance between two consecutive rows of crops is $2(L + D)$. This description is illustrated in Figure 1.

It is assumed that the geometries of the channels and the root distribution do not vary in the OY direction and are symmetrical about the planes $X = \pm k(L+D)$, for $k = 0, 1, 2, \cdots$. Water is supplied from the channels in uniform fluxes, v_0. However, on the soil surface outside the channels, the flux is zero. Given this situation, we wish to determine suction potential and the water uptake from the three different soil types stated above.

Because of the symmetry of the problem, it is sufficient to consider the semi infinite region defined by $0 \leq X \leq L + D$ and $Z \geq 0$. This region is denoted by R with boundary C. The boundary along the surface of the channel is denoted by C_1 and the surface of soil outside the channel by C_2. The boundary along $X = L+D$ is denoted by C_3, and C_4 is for $X = 0$. The fluxes over C_1 is v_0, while over C_2 is 0. There are no fluxes across C_3 and C_4 as the problem symmetrical about them. The derivatives $\partial\Theta/\partial X \to 0$ and $\partial\Theta/\partial Z \to 0$ as $X^2 + Z^2 \to \infty$.

3 Basic Equations

The governing equation of steady infiltration with root water uptake is given by

$$\frac{\partial}{\partial X}\left(K\frac{\partial\psi}{\partial X}\right) + \frac{\partial}{\partial Z}\left(K\frac{\partial\psi}{\partial Z}\right) - \frac{\partial K}{\partial Z} = S(X, Z, \psi), \tag{1}$$

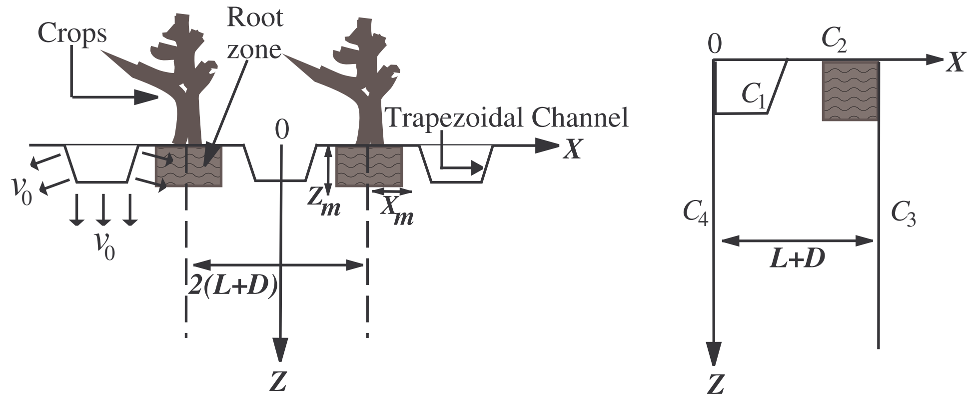

Figure 1: Geometry of periodic trapezoidal channels with roots zone

where K (LT^{-1}) is the hydraulic conductivity, ψ (L) is the suction potential, and S (T^{-1}) is the root water uptake function.

The relation between K and ψ is defined as

$$K = K_s e^{\alpha\psi}, \quad \alpha > 0, \tag{2}$$

where α (L^{-1}) is an empirical parameter and K_s is the saturated hydraulic conductivity. The Matric flux potential (MFP), Θ, is obtained using the Kirchhoff transformation

$$\Theta = \int_{-\infty}^{\psi} K ds. \tag{3}$$

Using equations (2) and (3), the following equation is obtained

$$\psi = \frac{1}{\alpha} \ln\left(\frac{\alpha\Theta}{K_s}\right), \tag{4}$$

and equation (1) is transformed to

$$\frac{\partial^2\Theta}{\partial X^2} + \frac{\partial^2\Theta}{\partial Z^2} - \alpha\frac{\partial\Theta}{\partial Z} = S\left(X, Z, \frac{1}{\alpha}\ln\left[\frac{\alpha\Theta}{K_s}\right]\right). \tag{5}$$

The flux normal to the surface with outward pointing normal $\mathbf{n} = (n_1, n_2)$ is given by

$$F = -\frac{\partial\Theta}{\partial X}n_1 + \left(\alpha\Theta - \frac{\partial\Theta}{\partial Z}\right)n_2. \tag{6}$$

The root water uptake function is as that in [15], which takes the form

$$S(X,Z,\psi)=\gamma(\psi)\frac{L_t\beta(X,Z)T_{pot}}{\int_0^{Z_m}\int_{L+D-X_m}^{L+D}\beta(X,Z)dXdZ}, \tag{7}$$

where γ is the root-water stress response function, L_t is the width of soil surface associated with the transpiration process, T_{pot} is the potential transpiration, and $\beta(X,Z)$ is the two-dimensional spatial root distribution, which takes the form

$$\begin{aligned}\beta(X,Z) &= \left(1-\frac{L+D-X}{X_m}\right)\left(1-\frac{Z}{Z_m}\right)\\ &\quad \times e^{-(p_Z/Z_m|Z^*-Z|+p_X/X_m|X^*-(L+D-X)|)},\\ &\quad L+D-X_m\le X\le L+D,\quad 0\le Z\le Z_m,\end{aligned} \tag{8}$$

where p_Z, p_X, X^*, and Z^* are empirical parameters.

Using the dimensionless variables

$$x=\frac{\alpha}{2}X,\quad z=\frac{\alpha}{2}Z,\quad \Phi=\frac{\pi\Theta}{v_0L},\quad f=\frac{2\pi}{v_0\alpha L}F,) \tag{9}$$

and the transformation

$$\Phi=e^z\phi, \tag{10}$$

equation (5) may be transformed to

$$\frac{\partial^2\phi}{\partial x^2}+\frac{\partial^2\phi}{\partial z^2}=\phi+\gamma^*(\phi)s^*(x,z)e^{-z}, \tag{11}$$

where

$$s^*(x,z)=\frac{2\pi}{\alpha L}\frac{l_t\beta^*(x,z)}{\int_0^{z_m}\int_{b-x_m}^{b}\beta^*(x,z)dxdz}\frac{T_{pot}}{v_0}, \tag{12}$$

and

$$\gamma*(\phi)=\gamma\left(\frac{1}{\alpha}\ln\left(\frac{\alpha v_0L\phi e^z}{\pi K_s}\right)\right). \tag{13}$$

Here

$$\begin{aligned} l_t &= \frac{\alpha}{2}L_t,\quad x_m=\frac{\alpha}{2}X_m,\quad z_m=\frac{\alpha}{2}Z_m,\quad x^*=\frac{\alpha}{2}X^*,\quad z^*=\frac{\alpha}{2}Z^*\\ p_x &= \frac{\alpha}{2}p_X,\quad p_z=\frac{\alpha}{2}p_Z,\quad a=\frac{\alpha}{2}L\quad b=\frac{\alpha}{2}(L+D),\end{aligned} \tag{14}$$

and

$$\begin{aligned}\beta^*(x,z) &= \left[1-\frac{b-x}{x_m}\right]\left[1-\frac{z}{z_m}\right]\\ &\quad\times e^{-(p_z/z_m|2z^*/\alpha-2z/\alpha|+p_x/x_m|2x^*/\alpha-2/\alpha\ (b-x)|)},\\ &\quad b-x_m\le x\le b,\quad 0\le z\le z_m.\end{aligned} \tag{15}$$

Equations (6), (9), and (10) yield

$$f = -e^{z}\left[\frac{\partial\phi}{\partial x}n_1 - \left(\phi - \frac{\partial\phi}{\partial z}\right)n_2\right]. \tag{16}$$

From equation (16), the normal derivative of ϕ may take the form

$$\frac{\partial\phi}{\partial n} = \phi n_2 - e^{-z}f. \tag{17}$$

Boundary conditions in term of ϕ are summarized as follows.

$$\begin{aligned}
\frac{\partial\phi}{\partial n} &= \frac{2\pi}{\alpha L}e^{-z} + n_2\phi, \text{ on the surface of the channels,} && (18)\\
\frac{\partial\phi}{\partial n} &= -\phi, \text{ on the surface of soil outside the channels,} && (19)\\
\frac{\partial\phi}{\partial n} &= 0, \quad x = 0 \text{ and } z \geq 0, && (20)\\
\frac{\partial\phi}{\partial n} &= 0, \quad x = b \text{ and } z \geq 0, && (21)
\end{aligned}$$

and

$$\frac{\partial\phi}{\partial n} = -\phi, \text{ as } z \to \infty. \tag{22}$$

An integral equation to solve equation (11), as discussed by Ang [2], is

$$\begin{aligned}
\lambda(\xi,\eta)\phi(\xi,\eta) &= \int\int_R \varphi(x,z;\xi,\eta)[\phi(x,z) + \gamma^*(\phi)s^*(x,z)e^{-z}]dxdz\\
&+ \int_C \left[\phi(x,z)\frac{\partial}{\partial n}(\varphi(x,z;\xi,\eta))\right.\\
&- \left.\varphi(x,z;\xi\eta)\frac{\partial}{\partial n}(\phi(x,z))\right] ds(x,z), && (23)
\end{aligned}$$

where

$$\lambda(\xi,\eta) = \begin{cases} \frac{1}{2}, & (\xi,\eta) \text{ lies on a smooth part of } C \\ 1, & (\xi,\eta) \in R \end{cases}, \tag{24}$$

and

$$\varphi(x,z;\xi,\eta) = \frac{1}{4\pi}\ln[(x-\xi)^2 + (z-\eta)^2] \tag{25}$$

is the fundamental solution of the Laplace's equation.

Integral equation (23) may be solved numerically using the dual reciprocity boundary element procedure with predictor corrector scheme as discussed in [15].

4 Results and Discussion

The method described in the preceding section is tested on problems involving infiltration from periodic identical trapezoidal channels into three different types of homogeneous soil with root water uptake process. We set $L = D = 50$ cm, and the width and the depth of the channels are $4L/\pi$ and $3L/2\pi$ respectively. The potential transpiration rate, T_{pot}, is 4 cm/d, which was also used by Li et al [10], and Šimunek and Hopmans [13] in their studies. The homogeneous soils considered in the present study are pima clay loam, touchet silt loam, and guelph loam. The values of experimental parameters α and K_s of the soils are as reported by Amozegar-Fard et al [1] and Bresler [6], and are summarized in Table 1.

Table 1: The values of α and K_s of three different homogeneous soils

Soil type	α	K_s
Pima clay loam	0.014 cm^{-1}	9.9 cm/d
Touchet silt loam	0.0156 cm^{-1}	41.99 cm/d
Guelph loam	0.034 cm^{-1}	31.71 cm/d

We assume that root zones have the same width and depth of 100 cm. We further assume that there are no fluxes across soil surface outside the channels, which means the soil surface has the lowest amount of water. Correspondingly, it is only reasonable to consider a root distribution which has low density at the surface of soil. As the roots go deeper into the soil, their density increases until it reaches a limit at a certain level of soil depth. From this level to the end point of the root zone in OZ direction, the root density decreases to zero. We also assume that the root distribution in the direction opposite to OX has the same pattern, which is similar to that assumed by Vrugt et al.

Typical parameter values for the root distribution described above are $X^* = 25$ cm, $P_X = 2.00$, $Z^* = 20$ cm, and $P_Z = 5.00$. The values of P_X, Z^*, and P_Z chosen are as reported by Vrugt et al [17]. The value of X^* is chosen half of X^* in the same report as the width of the root zone considered in this study is half of that in the report. Using this set of values, the densest part of the root distribution along Z-axis is at $Z = 20$ cm, and along X-axis is at $X = 75$ cm.

The root-water stress response function γ used here is identical to that reported by Utset et al [16], which can be seen graphically in Figure 2. The value of h_3 for $T_{pot} = 0.4$ cm/d is interpolated from $h_{3,a}$ and $h_{3,b}$, and we have $h_3 = -470$.

The DRBEM with the predictor-corrector scheme is employed to obtain numerical solutions to equation (11). Using the numerical solutions and equations (4), (9), and (10), numerical values of suction potential, ψ, are obtained. Substituting ψ to equation (7) yield values of root uptake function, S. To employ the DRBEM, the domain must be bounded by a simple closed curve. The domain is set to be between $z = 0$ and $z = 4$, sufficient depth for boundary conditions to

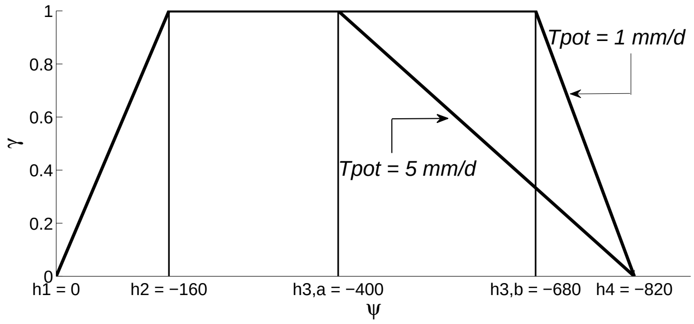

Figure 2: Graph of root-water stress response function reported by Utset et al.

be applied without significant impact to values of Φ in the domain. The number of line segments on the boundary is 202, and interior points chosen as collocation points are 619 points. These numbers of line segments and interior points are chosen in such a way, such that an optimum computational time and the convergence of the values of Φ are achieved after several computational experiments. Some of the results are presented graphically in Figures 3 to 7.

The values of ψ and S along Z-axis at $X = 60$ cm are shown in Figures 3(a) and 4(a) respectively. The result indicate that at $X = 60$ cm, ψ is an increasing function, which means the water content increases with soil depth. This is due to the condition specifying that there is no water flux on the soil surface, that is, the soil surface has the least water content. It can be seen that at any value of Z, the value of ψ in guelph loam is the highest among those in the other types of soil, and ψ in pima clay loam is the lowest, indicating that coarser soils yield higher value of ψ. Since the values of ψ are between -100 and -30, from Figure 2 higher ψ implies smaller value of response function, and hence smaller values of S as shown in Figure 4(a). This indicates that the amount of water absorbed by the roots from a finer soil is higher than those from coarser soils.

The values of S increases as Z increases, and reaches a peak value at $Z = 20$ cm. For $Z \geq 20$ cm, S is decreasing and $S = 0$ at $Z = 100$ cm. These results are expected as from $Z = 0$ to $Z = 20$ cm the root distribution increases, and from $Z = 20$ cm to $Z = 100$ cm the distribution decreases and no root at $Z \geq 100$ cm.

Figures 3(b) and 4(b) show the values of ψ and S at $X = 75$ cm respectively. As before, a coarser soil type yields higher value of ψ, but smaller value of S. The density of root distribution along OX-axis reaches a maximum at $X = 75$ cm, and from equation (8) the density is about 5 times at $X = 60$ cm. It can be seen that the uptake at $X = 70$ cm is much higher than that at $X = 60$ cm.

Figure 3(c) shows the values of ψ and Figure 4(c) shows the values of S at $X = 90$ cm. The density of root distribution at $X = 90$ cm is about 4/5 of that

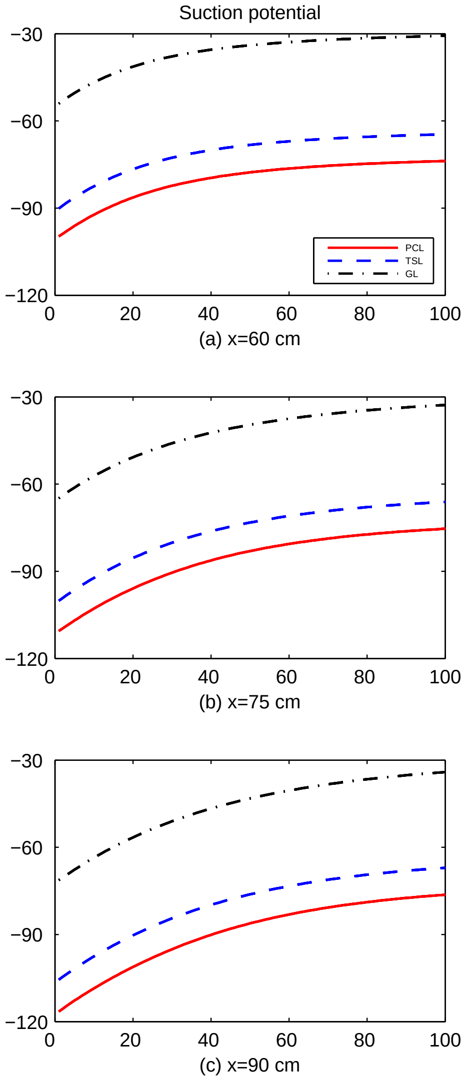

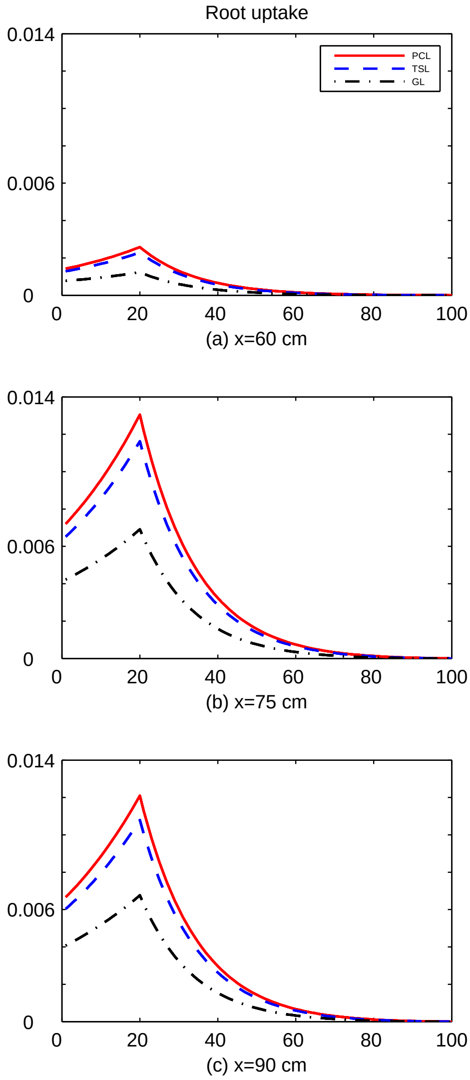

Figure 3: Suction potential in three different homogeneous soils, pima clay loam (PCL), touchet silt loam (TSL), and guelph loam (GL), at $x = 60$ cm, 75 cm, and 90 cm

Figure 4: Root-water uptake in three different homogeneous soils, pima clay loam (PCL), touchet silt loam (TSL), and guelph loam (GL), at $x = 60$ cm, 75 cm, and 90 cm

at $X = 75$ cm. The value of ψ at $X = 90$ cm is smaller than that at $X = 75$ cm, and this implies that values of response function at $X = 90$ are higher than those at $X = 75$ cm. From these, the values of S at $X = 90$ cm is almost the same as those at $X = 75$ cm.

Figures 5 to 7 show the distribution of root water uptake function values, S, in the root zone. Specifically, Figure 5 shows the distribution of the values of S in PCL. The distribution of the values of S in TSL and GL are shown in Figures 6 and 7 respectively. It can be seen that maximum uptake occurs at point (75 cm, 20 cm). This is expected, as the values of X^* and Z^* are 25 cm and 20 cm. It can also be seen that finer soils yield higher value of S than coarser soils over the root zone. These results indicate that the highest amount of water absorbed by the plant roots at the depth of 20 cm and 25 cm away from the plant in the X-direction, and the total amount of water absorbed from finer soil types is higher than that from coarser soils.

The amount of water absorbed by plant roots may be calculated using the formula

$$\int_0^{100} \int_{50}^{100} S(X, Z, \psi)\, dX dZ. \tag{26}$$

Since S is a function of ψ, and ψ is obtained numerically using the numerical method described in the preceding section, the integral in (26) cannot be evaluated analytically. Thus, a numerical scheme is used to estimate this integral.

To compute the integral numerically, the root zone is divided into 100×100 rectangular region. Let A_{ij} be the region at j-th row and i-th column, and Δ_{x_i} and Δ_{z_j} be the breadth and the length of region A_{ij}.

Let S_{ij} be the value of the root water uptake function at one corner of A_{ij}. Hence, integral (26) may be approximated using

$$\sum_{j=1}^{100} \sum_{i=1}^{100} S_{ij} \Delta_{x_i} \Delta_{z_j}. \tag{27}$$

Using formula (27), numerical values of the total amount of water absorbed over from PCL, TSL and GL are 12.07 cm^2/d, 10.79 cm^2/d and 6.52 cm^2/d. These numerical values indicate that crops absorb more water from finer soils than coarser soils.

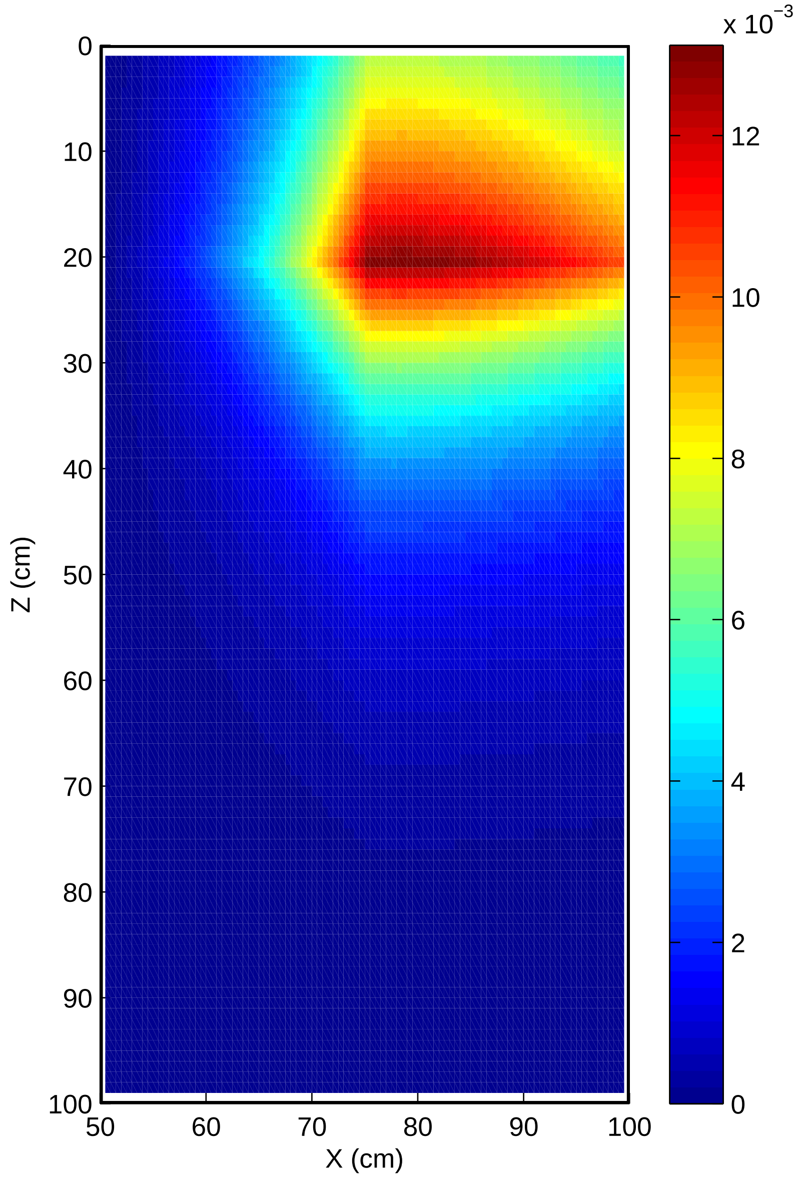

Figure 5: Surface plot of root uptake function over root zone for PCL

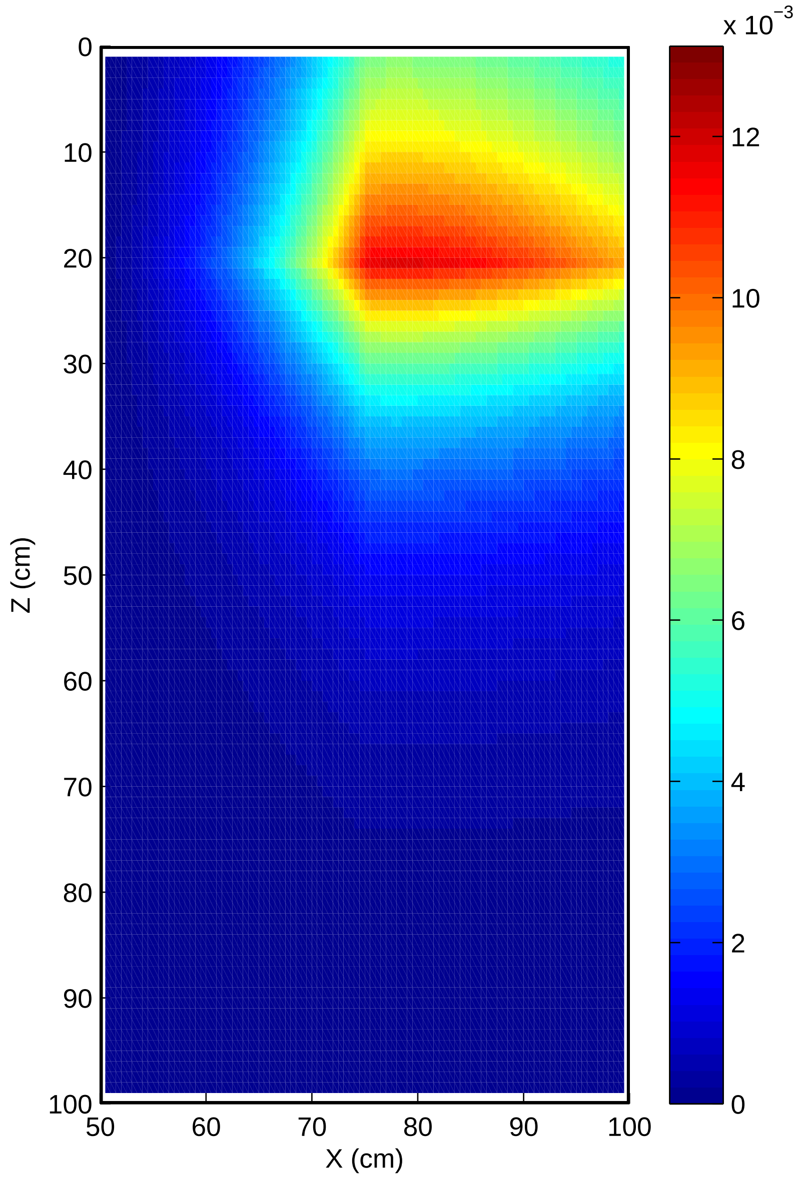

Figure 6: Surface plot of root uptake function over root zone for TSL

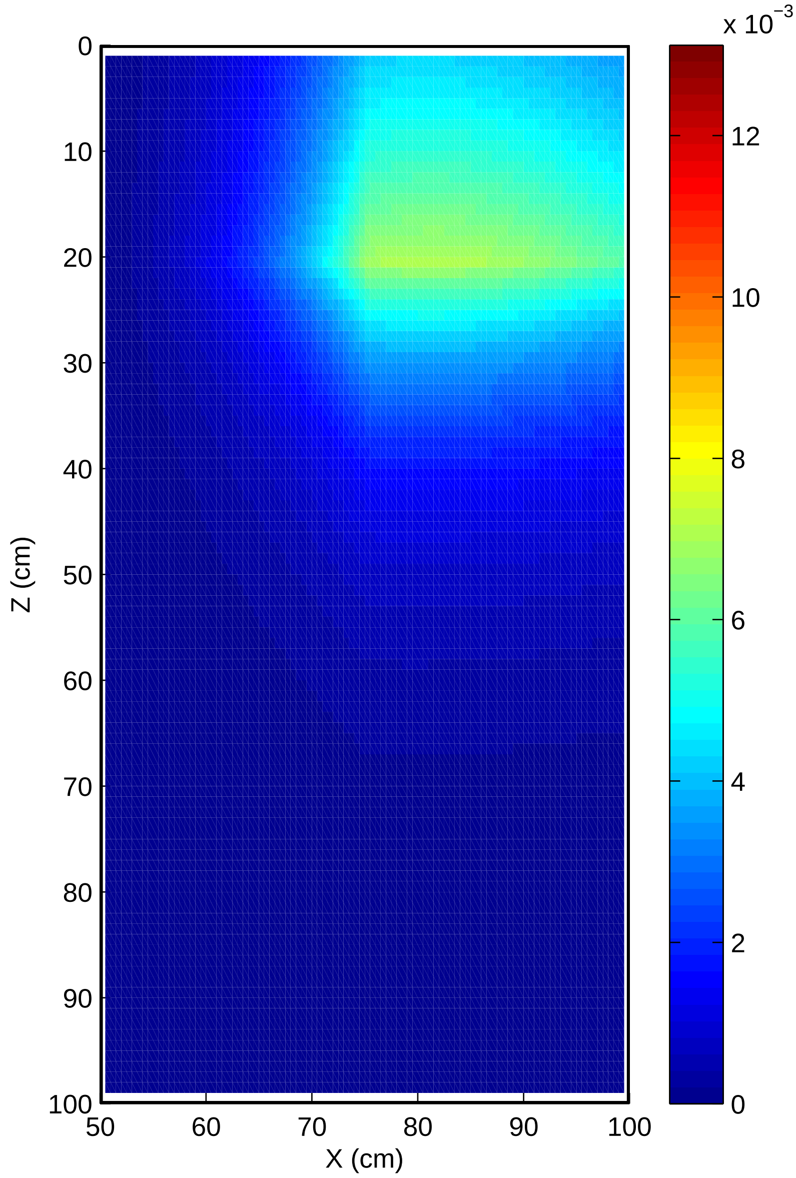

Figure 7: Surface plot of root uptake function over root zone for GL

5 Concluding Remarks

Problems involving steady infiltration from periodic trapezoidal channels with root-water uptake in three different types of homogeneous soil have been solved numerically. A DRBEM with a predictor-corrector scheme is employed to solve the problems. To predict the values of water stress response function, solutions for corresponding problems without root water uptake are needed, and then employing the predictor-corrector scheme together with the DRBEM the required values of the function is obtained. Using these values, numerical solutions of the dimensionless MFP are obtained. Using the dimensionless MFP and empirical parameters, suction potential can be calculated. Furthermore, water uptake can be obtained.

In this study, the results indicate that coarser soil types generally provide higher suction potential than finer soil. In contrast, coarser soil types results in lower uptake of moisture than finer soil type.

Acknowledgment

Imam Solekhudin wishes to thank the Directorate General of the Higher Education of the Republic of Indonesia (DIKTI) for providing financial support for this research.

References

[1] Amoozegar-Fard, A., Warrick, A. W. and Lomen D. O., Design Nomographs for Trickle Irrigation System, *J. of Irrigation and Drainage Engineering*, **110**, 107 - 120, 1984.

[2] Ang, W. T., *A Beginer's Course in Boundary Element Method*, Universal Publishers Boca Raton, Florida, 2007.

[3] Azis, M. I., Clements, D. L. and Lobo, M., A Boundary Element Method for Steady Infiltration from Periodic Channels, *ANZIAM J.*, **44(E)**, C61 - C78, 2003.

[4] Basha, H. A., Multidimensional Linearized Nonsteady Infiltration Toward A Shallow Water Table, *Water Resource Research*, **36**, 2567 - 2573, 2000.

[5] Batu, V., Steady Infiltration from Single and Periodic Strip Sources, *Soil Sci. Soc. Am. J.*, **42**, 544 - 549, 1978.

[6] Bresler, E., Analysis of Trickle Irrigation with Application to Design Problems, *Irrigation Science*, **1**, 3 - 17, 1978.

[7] Clements, D. L., Lobo, M. and Widana, N., A Hypersingular Boundary Integral Equation for a Class of Problems Concerning Infiltration from Periodic Channels, *El. J. of Bound. Elem.*, **5**, 1 - 16, 2007.

[8] Clements, D. L. and Lobo, M., A BEM for Time Dependent Infiltration from An Irrigation Channel, *Engineering Analysis with Boundary Elements*, **34**, 1100 - 1104, 2010.

[9] Gardner, W. R., Some Steady State Solutions of the Unsaturated Moisture Flow Equation with Application to Evaporation from a Water Table, *Soil Sci.*, **85**, 228 - 232, 1958.

[10] Li, K. Y., De Jong, R. and Boisvert, J. B., An Exponential Root-Water-Uptake Model with Water Stress Compensation, *J. of Hydrol.*, **252**, 189 - 204, 2001.

[11] Lobo, M., Clements, D. L. and Widana, N., Infiltration from Irrigation Channels in a soil with Impermeable Inclusions, *ANZIAM J.*, **46(E)**, C1055 - C1068, 2005.

[12] Lobo, M. and Clements, D. L., Boundary Element Methods for Infiltration from Irrigation Channels, *Advances in Boundary Element Techniquaes VI*, 235 - 240, 2005.

[13] Šimunek, J. and Hopmans, J. W., Modeling Compensated Root Water and Nutrient Uptake, *Ecol. Model.* (2008), doi:10.1016/j.ecolmodel.2008.11.004.

[14] Skaggs, T. H., van Genuchten, M. T., Shouse, P. J. and Poss J. A., Macroscopic approaches to root water uptake as a function of water and salinity stress, *Potato Res.*, **43**, 19 - 29, 2000.

[15] Solekhudin, I. and Ang, K. C., A DRBEM with A Predictor-Corrector Scheme for Steady Infiltration from Periodic Channels with Root-Water Uptake, *Engineering Analysis with Boundary Elements*, **36**, 1199 - 1204, 2012.

[16] Utset, A., Ruiz, M. E., Garcia, J. and Feddes, R. A., A SWACROP-based potato root water-uptake function as determined under tropical conditions, *Potato Res.*, **43**, 19 - 29, 2000.

[17] Vrugt, J. A., Hopmans, J. W. and Šimunek, J., Calibration of a Two-Dimensional Root Water Uptake Model, *Soil Sci. Soc. Am. J.* **65**, 1027 - 1037, 2001.

[18] Vrugt, J. A., van Wijk, M. T., Hopmans, J. W. and Šimunek, J., One-, Two-, and Three-Dimensional Root Water Uptake Functions for Transient Modeling, *Water Resources Res.* **37**, 2457 - 2470, 2001.

[19] Waechter, R. T. and Mandal, A. C., Steady Infiltration from A Semicircular Cylindrical Trench and A Hemispherical Pond into Unsaturated Soil, *Water Resources Res.* **29**, 457 - 467, 1993.